Check for updates

Bamboo fiber reinforced polypropylene composites for transportation applications

Sanjita Wasti[1], Surbhi Kore[1], Pritesh Yeole[1], Halil Tekinalp[2], Soydan Ozcan[2] and Uday Vaidya[1,3,2]*

[1]Tickle College of Engineering, University of Tennessee, Knoxville, TN, United States, [2]Manufacturing Sciences Division, Oak Ridge National Laboratory, Oak Ridge, TN, United States, [3]Institute for Advanced Composites Manufacturing Innovation (IACMI), Knoxville, TN, United States

The Apitong wood species has long been the most popular choice for transportation, such as in trailer decking and shipping container floors. However, Apitong is depleting due to its excessive usage. Bamboo fiber provides as an alternative due to its low density ($608-780 \, kg/m^3$) and lightweight attributes. This study explores 1) development and properties of bamboo-thermoplastic composites with different fiber content, and 2) application of bamboo composite in trailer decking (a transportation application) as an alternative to Apitong. Extrusion-compression and compression molding was used as processing approaches for the bamboo-thermoplastic composites. The basic panels were tested for flexural loading and nail pull out to evaluate the feasibility as a viable trailer decking material. The flexural strength and modulus of bamboo composite were found to be 17 and 98% higher than Apitong, respectively. The density of the bamboo-thermoplastic was $670 \, kg/m^3$ compared to Apitong ($737 \, kg/m^3$), hence 10% lighter. The nail pull-out strength was comparable between the two. The work progressed to producing prototype trailer decking members via extrusion-compression and compression molding. The bamboo-composite decking was evaluated on a trailer test bed and exhibited excellent surface wear response, minimal internal damage and withstood 400 fatigue cycles with onset of failure only at the supports, which the span did not exhibit damage.

KEYWORDS

bamboo fibers, extrusion compression molding, overmolding, sandwich composite, trailer decking, apitong, nail pull out

1 Introduction

The fundamental requirements of material selection for truck/trailer decking elements are high strength and high stiffness to weight ratio, excellent corrosion resistance, luminescence, adequate nail pull out strength (typically nails are used to secure cargo), fatigue and impact resistance, ease of installation, and superior durability (Osei-Antwi et al., 2014). The global truck trailer market was $350 billion in 2020 and is forecasted to grow at a compound annual growth rate (CAGR) of 6.18% by 2026 (Global Truck, 2022 Trailer Market to 2026–by Application Type, Truck Tonnage Capacity,

FIGURE 1
Schematic representing use of hardwood for truck trailer decking application.
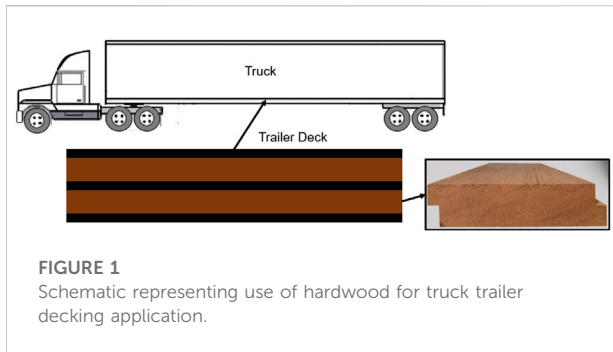
Trailer Type, Vehicle Type and Region). The Apitong (Dipterocarpus grandifloras) species of hardwood is widely used for trailer decking in trucks (Figure 1) and shipping container floors due to their excellent mechanical properties (Our Apitong | Terradeck, 2022; Slaven et al., 2022). Apitong exhibits 20% higher modulus of elasticity (15.81 GPa) and 25% higher crushing strength (61.4 MPa) as compared to American Oak (Our Apitong | terradeck. id). Due to the habitat loss and its excessive use as lumber, the supply of Apitong is dwindling, resulting in increased price (Slaven et al., 2022). Further, the International Union for Conservation of Nature (IUCN) has red listed Apitong as a threatened species (Khademibami et al., 2021; Slaven et al., 2022). There is hence an urgent need to search for alternative material(s) to replace Apitong in trailer decking applications.

Conventional fiber reinforced polymer (FRP) composites can fulfill structural durability requirements due to their excellent mechanical properties, fast production rate and superior durability. The growth of FRP composites is exponential in automotive, aerospace, wind turbine, sports, and civil infrastructure sectors. The global consumption of FRP composites for decking is 20% (Duflou et al., 2012; Ali et al., 2021). Thermoset polymers such as polyester, vinyl ester, and epoxies are common polymers used in decking applications. Reinforcements such as carbon, glass, aramid, basalt, and natural fibers including bamboo, jute, flax and hemp fibers are of interest in decking applications (Guo et al., 2021).

Natural fiber composites are gaining attention because they are environmental friendly, sustainable and biodegradable materials with superior vibration and noise damping properties than synthetic fibers (Mohanty et al., 2018). Natural fiber composites (NFC) have high strength-to-weight and stiffness-to-weight ratio, compared to E-glass fiber composites (Duflou et al., 2012). NFC market was 4.46 billion USD at 2016 and the CAGR is projected to increase by 11.8% by 2024 (Rajendran Royan et al., 2021).

Bamboo fiber (BF) is one of the commonly used natural fiber for reinforcing the composites due to its abundance, short growth cycle (only couple of months) and high strength with respect to

weight (Ibrahim et al., 2015; Mousavi et al., 2022). Compared to some natural fibers such as coir, sisal and jowar, BF has lower density (608–780 kg/m^3) and higher tensile strength (140–800 MPa) and modulus (11–46 GPa) (Ratna Prasad and Mohana Rao, 2011; Lotfi et al., 2021). In the past, several studies were done with the different forms of bamboo (dust, fiber and strips) reinforced composites (Abdul Khalil et al., 2012; Ibrahim et al., 2015; Mousavi et al., 2022). Ratna Prasad and Mohana Rao, 2011 studied the mechanical properties of bamboo, sisal and jowar fiber reinforced polyester composites where they found that for 0.4 volume fraction of fiber content, bamboo fiber reinforced composites had highest tensile strength of 126.2 MPa followed by jowar fiber reinforced composites (124 MPa) and sisal fiber reinforced composites (65.5 MPa) whereas tensile modulus was highest for jowar fiber reinforced composites (2.75 GPa) followed by bamboo fiber composites (2.48 GPa) and sisal fiber composites (1.90 GPa). Authors also performed flexural test where they observed superior flexural strength and modulus (at 0.4 volume fraction of fiber) of jowar fiber composites (flexural strength-134 MPa, modulus-7.87 GPa) followed by bamboo fiber composites (flexural strength-128.5 MPa, modulus- 3.70 GPa and sisal fiber composites (flexural strength-99.5 MPa, modulus- 2.49 GPa). Wei et al. (2022) examined BF-concrete composites with the thread reinforcement connections and its shearing effect on mechanical properties. They reported that the cross-sectional load bearing reduced by 0.8 and flexural properties increased 3.7 times for BF-concrete composites. Rassiah et al. (2014) studied the mechanical properties of BF strips (1.5–2.5 mm thick) reinforced in unsaturated polyester (UP) composites. Their results showed that the 2.5 mm thickness BF strips reinforced in UP showed tensile stress, tensile modulus, flexural modulus, and Charpy impact strength of 49 MPa, 3,897 MPa, 5,208 MPa, and 4.2 J/mm^2, respectively whereas that by pure BF strips was 43, 2990, 3,831 MPa, and 3 J/mm^2 respectively. The mechanical properties illustrates that laminated UP-BF strips provided superior strength than pure BF strips (Rassiah et al., 2014). Furthermore, BFs are also used as reinforcement in polyolefins such as polyethylene (PE) and polypropylene (PP) due to high stiffness-to-weight, strength-to-weight and superior creep resistance. However, the significant differences between hydrophobic and hydrophilic behavior of PP and BF results in reduced mechanical strength of the composite due to poor interfacial adhesion between the fiber and matrix (Thwe and Liao, 2003; Lee et al., 2009). Hence, various techniques have been used to overcome the interfacial strength challenges such as—1) alkaline treatment to extract the lignin from BF surface (Deshpande et al., 2000; Das and Chakraborty, 2008), 2) blending BF with either synthetic fiber (glass fiber, carbon fiber etc.) or natural fibers (flax, kenaf etc.) to enhance the mechanical properties of bamboo composites (Fang et al., 2015; Chee et al., 2019) and 3) addition of a coupling agent such as maleic

anhydride PP (MAPP), where the surface of the PP is modified through graft polymerization (Lee et al., 2009).

Most of the investigations on BF composites have used extrusion, injection and compression molding, and/or hand lay-up processes (Guo et al., 2021; Slaven et al., 2022). There is limited research conducted on the overmolding process for BF composites, where overmolding can be considered as a hybrid manufacturing technique. Overmolding is an emerging manufacturing approach in automotive and aerospace where a continuous fiber reinforcement is selectively used in areas over discontinuous fiber intermediates to reduce cost yet obtain high load bearing performance. Overmolding is adopted to fabricate high-performance light-weight advanced composite parts through a single step process. This technique can be beneficial to reduce waste and energy consumption (Aliyeva et al., 2021).

The primary objective of this work was to develop bamboo bio-composites as possible alternative to Apitong for trailer decking application. PP-BF composites with varying content of BF were prepared using the extrusion compression molding (ECM) technique. Bamboo strips (BS) were overmolded with PP-BF to form trailer decking panels. The properties of BF reinforced PP and overmolded trailer decking panels were investigated using mechanical, thermal and morphological characterization techniques. The baseline work was extended to prototyping a BF-PP overmolded trailer deck component. Field tests on prototype trailer deck panels were conducted to evaluate their performance.

2 Materials and methods

2.1 Materials

PP pellets (ExxonMobil™ PP3155 homopolymer) of density $900 \, kgm^{-3}$ and melting temperature of $170°C$ were procured from Exxon Mobil Corporation. BF, BS and Apitong were provided by Resource Fiber Inc., Homewood, Alabama, USA. BF used in this study was in the range of 0.2–7 mm in length.

2.2 Compounding and extrusion compression molding of BF-PP composites

Compounding of PP and BF into a composite pellet was done using a Gala line twin screw compounder (model # 6–8.1) (Gala Industries, VA). PP pellets were fed through the primary gravimetric feeder whereas BF was fed through the secondary gravimetric feeder. Temperature of zone 1 to zone 9 of the twin screw were set at 80 , 140, 165, 165, 190, 180, 180, 180 and 180°C respectively and the screw speed was set at 250 rpm. Compounded PP-BF was then passed through a 12-hole strand die, attached at the end of the extruder which was then quenched in water and chopped into pelletized form using

motorized chopper blades. The content of BF was varied from 5, 10, 15 and 20 wt.%. From here on specimens with 5, 10, 15 and 20 wt.% BF reinforced PP are noted as PP-BF-5, PP-BF-10, PP-BF-15 and PP-BF-20 respectively.

PP-BF pellets prepared via the twin-screw extruder were fed through a low shear single screw B-20 Impco Plasticator to obtain a molten charge. Zone 1, Zone 2, Zone 3, and Zone 4 of the plasticator were set at 190 , 195, 200, and 205°C respectively. The hot plasticized BF-PP charge was then pressed using 100-ton Beckwood hydraulic compression press at a pressure of 20 tons for 3 min dwell time. These steps are referred to extrusion compression molding (ECM). Figure 2 illustrates the process flow of ECM of BF and PP. The composite panels prepared from various concentrations of BF and PP were used for further characterization.

2.3 Preparation of trailer deck prototype of PP-BF-BS composites

For trailer decking panels it was deemed necessary to produce thick section panels for flexural load bearing. Sandwich composite design(s) have been applied to marine decks, aerospace floor components, and building infrastructure due to their potential for lightweight and high bending resistance.

Sandwich composites comprise a low density core sandwiched between two stiff facesheets and offer potential for significant weight and energy savings (Honeycomb Sandwich Design Technology–Hexcel.com, 2022). Facesheets are bonded to the core with an adhesive and support the out-of-plane bending as well as in-plane loads. The core provides the flexural stiffness and out-of-plane shear and compressive strength (Honeycomb Sandwich Design Technology–Hexcel.com, 2022). In most applications, polyurethane or poly vinyl chloride foam or balsa wood are used as the core of a sandwich and the facesheets consist of fiber reinforced polymer (FRP) materials. The core also performs the function of providing insulation against heat, sound and vibration. In this study, bamboo strips were used as core and the facesheets (skins) comprised ECM PP-BF, the design providing the benefits of the sandwich composite construction.

A comparison of a sandwich composite with a monocoque construction shown in Figure 3, illustrating the effectiveness of a sandwich design. The sandwich composite is comprised of two identical facesheets of thickness t and a core depth of c. The monocoque construction is a flat sheet composite of thickness $2t$, and hence approximately the same weight as that of the sandwich composite in Figure 3A. The weight of the core is neglected.

The extensional stiffness (K) per unit width of both the constructions in Figure 3 is given by:
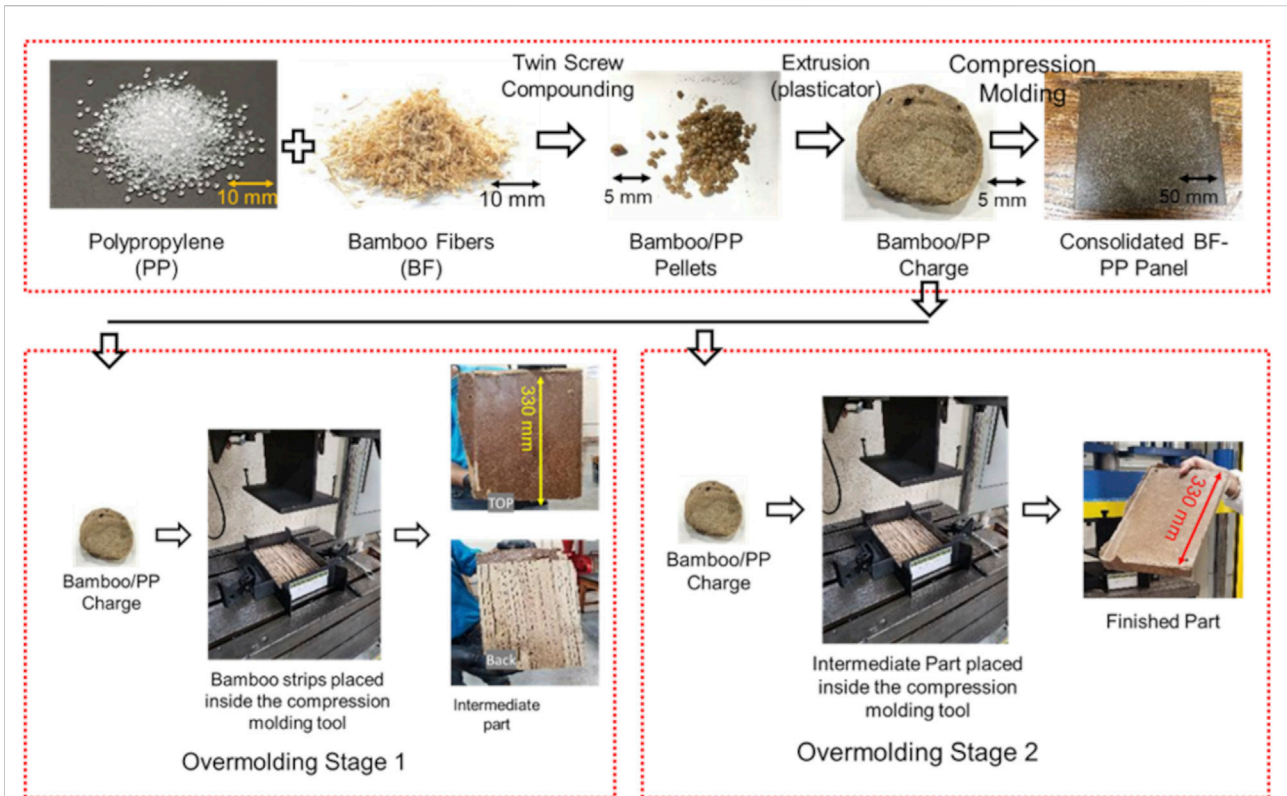
FIGURE 2
Process flow for extrusion compression molding of PP-BF composites and ECM of PP-BF-BS composite for trailer decking.
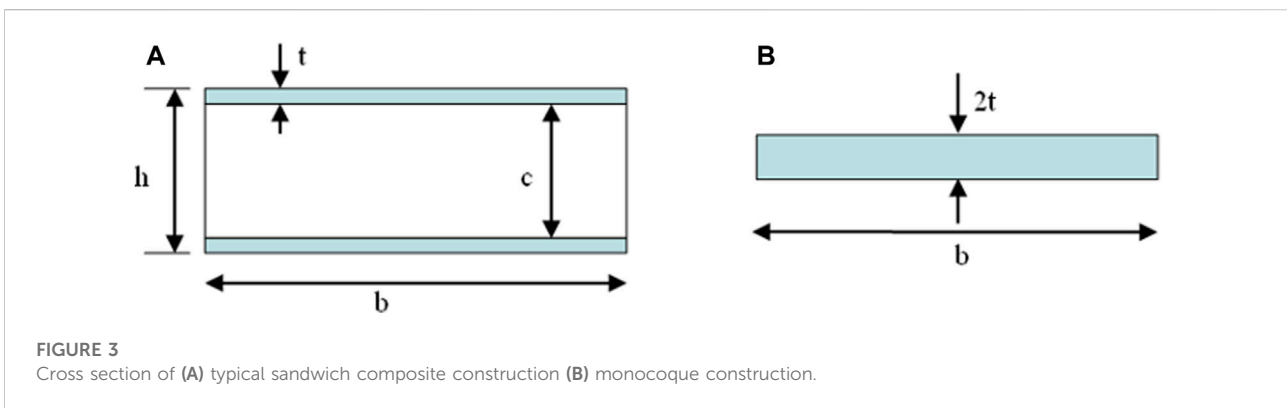

FIGURE 3
Cross section of **(A)** typical sandwich composite construction **(B)** monocoque construction.

$$K = \frac{2E_f t}{\left(1 - v_f^2\right)} \quad (1)$$

where E_f is the modulus of the facesheet and v_f is the volume fraction of the facesheet material. For in-plane tensile and compressive loads both constructions have the same in-plane stiffness. However, there is a marked difference in the flexural stiffness (per unit width) for the two types. The flexural

stiffness for the monocoque construction shown in Figure 3B is:

$$D_{monocoque} = \frac{2E_f t^3}{3\left(1 - v_f^2\right)} \quad (2)$$

The flexural stiffness for the isotropic foam core sandwich composite is given by:

$$D_{sandwich} = \frac{E_f t c^2}{2\left(1 - v_f^2\right)} \qquad (3)$$

From these equations it can be seen that the ratio of flexural stiffness of foam core sandwich to a monocoque construction of approximately the same weight, using the same facesheet material is:

$$\frac{D_{sandwich}}{D_{monocoque}} = \frac{3}{4}\left(\frac{c}{t}\right)^2 \qquad (4)$$

As an example, if $t/c = 1/20$, then the flexural stiffness of the sandwich construction is 300 times the flexural stiffness of the monocoque construction. Due to this the sandwich panel exhibits lower lateral deflection, higher overall buckling loads and lightweight advantages over the monocoque construction of nearly the same weight (Honeycomb Sandwich Design Technology–Hexcel.com).

Trailer decking sandwich panel(s) was prepared by overmolding process which includes PP-BF-20 as skin (jacket) and BS as the core. Overmolding process was conducted in two steps. In the first step, BS were placed in the flat mold (330 mm × 203 mm) mounted in a Beckwood Hydraulic press and a charge of BF-PP was produced using ECM process (as mentioned in Section 2.2). The molten charge then transferred to the mold and placed on top of BS. A pressure of 20 tons was applied for 3 min dwell time. With increase in the pressure, molten charge flowed within the tool and formed an excellent bond with BS. In order to create PP-BF skin on the other side (step 2), the compressed panel was flipped and the previous step 1 was repeated. From here on, BS over molded PP-BF-20 is referred as PP-BF-BS. Figure 2 illustrates the process of preparing PP-BF-BS composite trailer decking panel.

2.4 Characterization

2.4.1 Thermogravimetric analysis

The effect of fiber content on the thermal stability of the PP-BF composites was determined using the Mettler 840 TGA (Columbus, OH). Samples were heated from room temperature to 600°C at the heating rate of 10°C/min under the nitrogen atmosphere.

2.4.2 Mechanical characterization
2.4.2.1 Tensile test

Tensile properties of the PP-BF composite panels were determined according to the ASTM D3039 standard. Five specimens of average dimension 255.2 mm × 24.8 mm × 3.2 mm were extracted from each PP-BF molded plaque. The tensile test was conducted using a Test Resources universal testing machine (Model 313 series frame, MN) with 50 kN load cell capacity. Extensometer was employed to tensile samples for monitoring the strain.

2.4.2.2 Flexural test (Three-point bend test)

Three-point bend test was performed on the specimens extracted from PP-BF and PP-BF-BS composite panels according to ASTM D790. The flexural test was conducted using a Test Resources universal testing machine (Model 313 series frame, MN) with 50 kN load cell capacity.

2.4.2.3 Izod test

For Izod impact characterization, specimens of dimensions 64 × 12 × 3.4 mm^3 were cut and notched in accordance with ASTM D256 from PP-BF composite panels. Tinius Olsen IT-504 impact pendulum tester with a loading capacity of 22.6J and 27N pendulum weight was used for testing the impact properties of samples. Five specimens for each sample were tested.

2.4.2.4 Nail pull-out test

Cargo and dunnage are often nailed to the decks to make it secure. So, the nail pull-out test is one of the critical tests that need to be performed on the material prepared/selected for truck/trailer decking applications. A nail pull-out test was performed on PP-BF-BS panel and an Apitong panel. A standard nail of 3.785 mm (0.149 in) diameter was driven into the plank. The nail-panel test specimen was housed in a Test Resources Universal Testing Machine (Model 313 series frame, MN) and subjected to tension at a low-test speed of 0.1 mm/min. Figure 4 illustrates the experimental setup of the nail pull-out test.

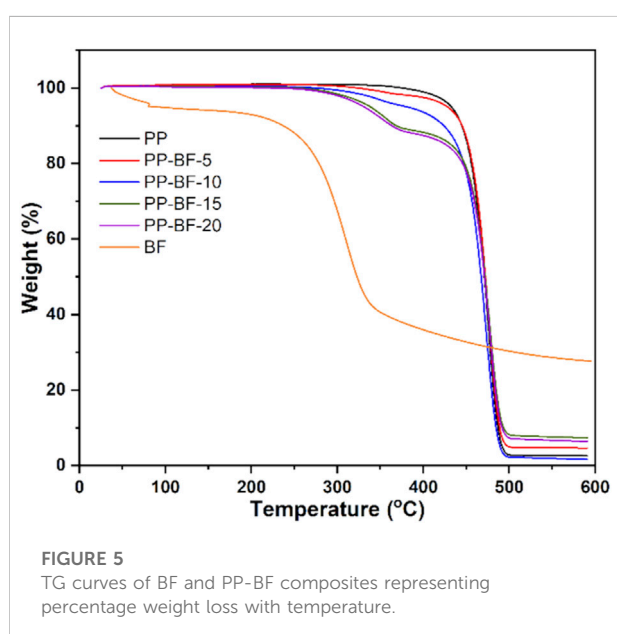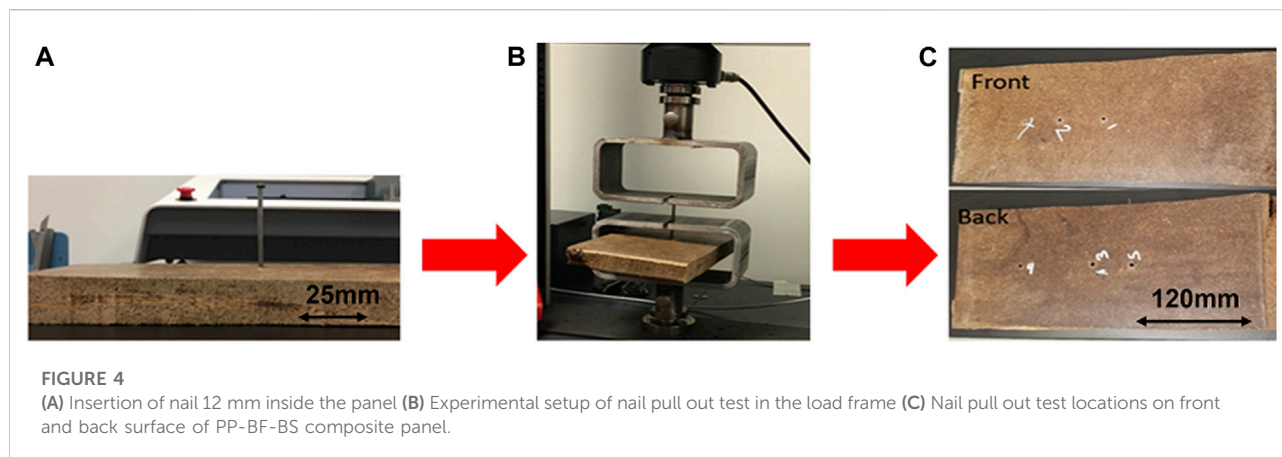### 2.4.3 Scanning electron microscopy

Morphological properties of tensile and flexural fractured samples were studied using Leo 1,525 scanning electron microscope (LEO Electron Microscopy Inc., Thornwood, NY). 5kV working voltage was used to study the fractured surfaces.

3 Result and discussion

3.1 Thermogravimetric analysis

Thermogravimetric (TG) curves of BF, neat PP and PP with varying content of BF are shown in Figure 5. TG curve of bamboo exhibits a multi-step degradation. Initial degradation by 7–8% occurred at ~100°C which was due to the moisture evaporation from the fibers. The second degradation occurred between 200–350°C due to decomposition of cellulose and hemicellulose and final degradation was observed from 350–450°C due to lignin decomposition. Zhang et al. (2018) and Chin et al. (2020) observed a similar trend of weight loss for BF.

For neat PP, degradation occurred in the range of 400–480°C. TG curves in Figure 5 show that increase in BF content reduced the onset temperature of the composites. TG curves of 15 and 20 wt.% BF reinforced composites clearly exhibited two step

FIGURE 4
(A) Insertion of nail 12 mm inside the panel **(B)** Experimental setup of nail pull out test in the load frame **(C)** Nail pull out test locations on front and back surface of PP-BF-BS composite panel.

FIGURE 5
TG curves of BF and PP-BF composites representing percentage weight loss with temperature.

bio-composites where first degradation was due to degradation of the fiber constituents and the second due to decomposition of LLDPE. Table 1 summarizes the temperatures at 5 ($T_{5\%}$), 10 ($T_{10\%}$) and 50% ($T_{50\%}$) weight loss of the samples during heating. With the addition of BF, $T_{5\%}$ and $T_{10\%}$ decreased, which was due to degradation of BF (since maximum degradation of BF was observed in the range of 350–450°C). However, there was no significant variation in $T_{50\%}$ with increase in BF. At 590°C, PP-BF-15 sample had highest residue or char content followed by PP-BF-20, PP-BF-5, PP and PP-BF-10. Despite the higher fiber content in PP-BF-20 and PP-BF-10 compared to PP-BF-15 and PP-BF-5 respectively, residual char of these samples is lower. The reason behind this might be the variation in the degradation rate of the lignin of BF, as lignin has complex structure and has slow and difficult decomposition ranging till 700°C (Yusoff et al., 2021). Additionally, difference in the chemical composition in BF might result in such variation (Yusoff et al., 2021). Comparative summary of amount of residue or char at 590°C of all the samples are presented in Table 1.

TGA study was conducted to evaluate the thermal stability of the material i.e., the maximum temperature up to which the material can withstand without dissociation/decomposition into its components (Yeole et al., 2018). As seen from the Figure 5, BF starts degradation from 200°C, processing temperature for each zone of each processing methods, (i.e., twin screw compounding versus ECM) was kept less

degradation. The first step was due to degradation of BF constituent and the others due to degradation of PP. Hidalgo-Salazar and Correa (2018) observed similar multi-step degradation of linear low density polyethylene (LLDPE)-Fique

TABLE 1 Temperatures at 5, 10 and 50% weight loss of the samples and residue (%) at 590°C obtained from TGA.

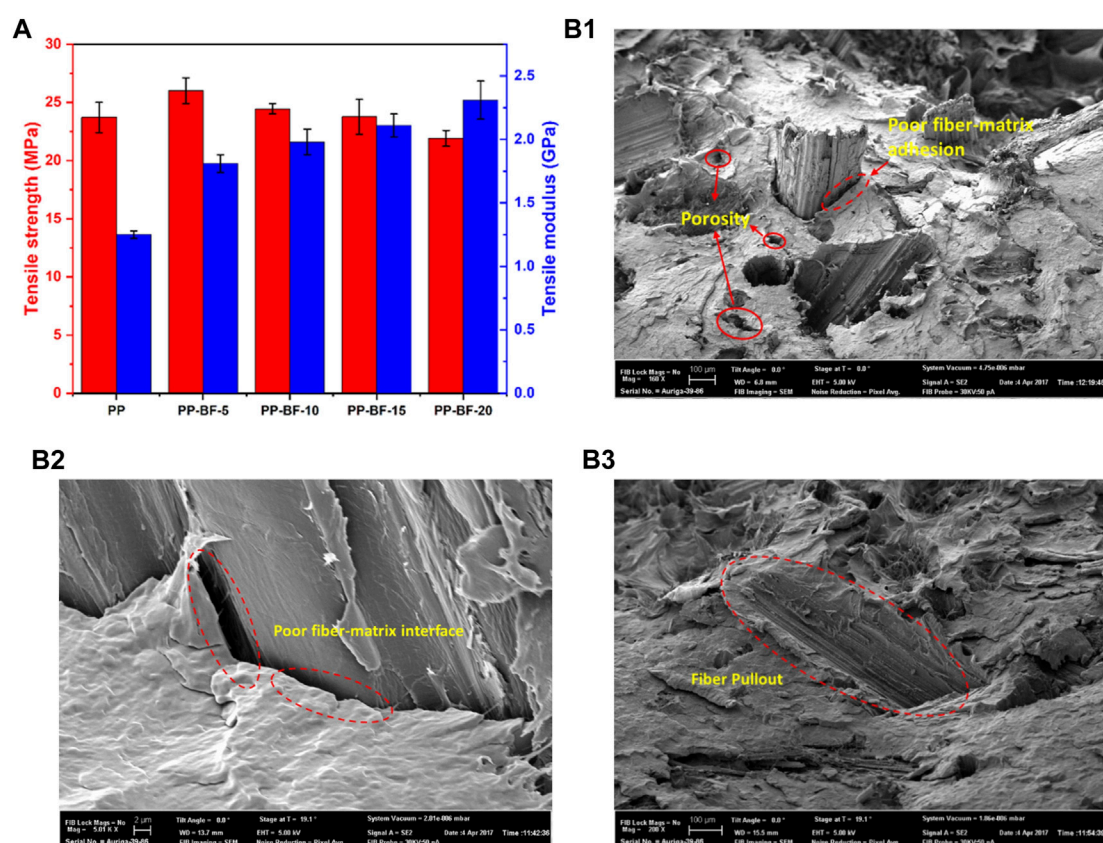| Samples	$T_{5\%}$ (°C)	$T_{10\%}$ (°C)	$T_{50\%}$ (°C)	Residue at 590°C (%)
PP	433	445	471	2.59
PP-BF-5	428	445	472	4.63
PP-BF-10	381	423	469	1.66
PP-BF-15	338	369	472	7.39
PP-BF-20	331	363	471	6.41

FIGURE 6
(A) Tensile properties of BF reinforced PP composites; **(B)** SEM images of tensile fractured samples indicating—**(B1)** poor fiber matrix adhesion, porosity **(B2)** poor fiber matrix adhesion and **(B3)** fiber pull-out.

than 200°C except the plasticator knife temperature (205°C), which was only 5°C more than onset decomposition temperature. The material was extruded immediately after it reached the knife, which can be interpreted that there was not sufficient time for material degradation.

3.2 Mechanical characterization

The mechanical characterization was conducted for BF-PP composites (Section 3.2.1) and PP-BF-BS sandwich composites (Section 3.2.2) respectively.

3.2.1 BF-PP composites
3.2.1.1 Tensile properties

The results of tensile testing of neat PP and PP with 5, 10, 15 and 20% by wt. of BF are presented in Figure 6A. Tensile strength and modulus of PP increased by 10 and 45% respectively with 5 wt.% addition of BF. On further addition of BFs i.e., 10%, 15% and 20wt.%, the tensile strength decreased. Rahman et al. (2010) also observed decrease in tensile strength of PP-sawdust

composites by 15% with increase in fiber content to 30 wt.%. BF are hydrophilic in nature and are not compatible with hydrophobic PP which results in poor fiber-matrix interfaces, as shown in Figures 6B1,B2. Figure 6B3 shows fiber pull out due to poor fiber-matrix adhesion. Weak interfacial properties of fiber and matrix influences negatively on the tensile strength of the composites (Bajpai et al., 2012; Gholampour and Ozbakkaloglu, 2020). With increase in fiber content, additional sites for weak interface increase, resulting in decrease in tensile strength (Bajpai et al., 2012). In contrast, tensile modulus increased with addition of BF and showed 20 wt.% BF had 79% higher modulus (2.31 GPa) as compared to neat PP (1.29 GPa). Lee et al. (2009) also observed increase in tensile modulus of PP from 0.44 to 1.31 GPa on reinforcing PP with 50wt% of BFs. In addition to the interfacial properties, tensile properties of the composite also depend on the fiber length. Longer fibers (fiber length > critical fiber length (Ning et al., 2020)) contribute to enhancement of strength, modulus and impact. However, shorter fibers (fiber length < critical fiber length) only enhance the modulus of the composites (Wang et al., 2018). BFs used in this study were in the range of 0.2–7 mm
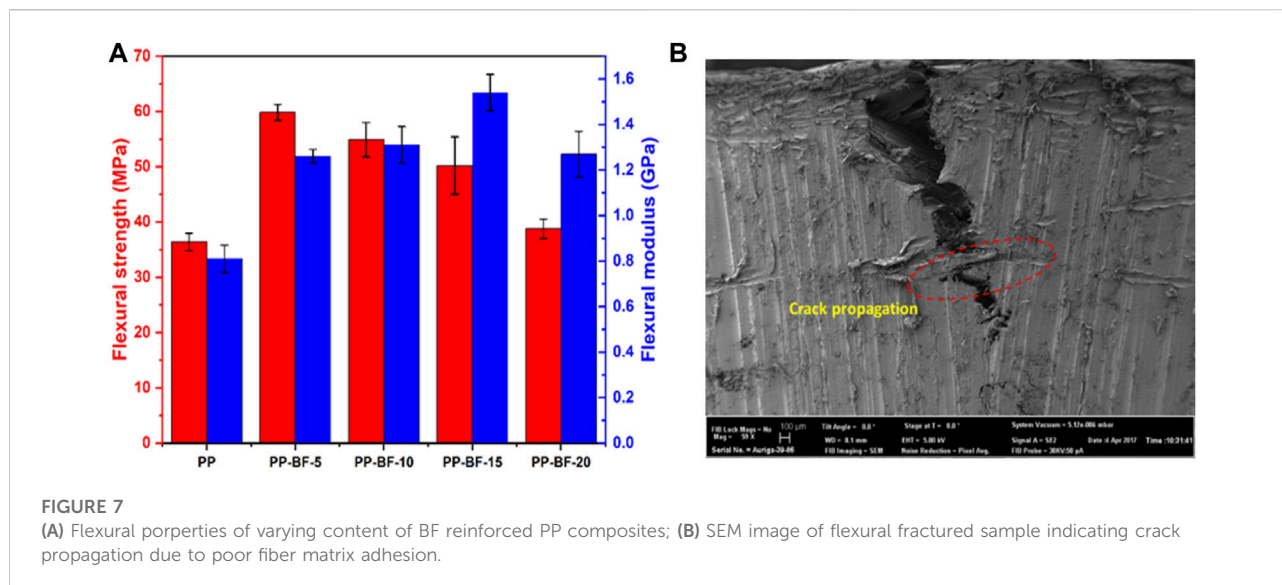
FIGURE 7
(A) Flexural porperties of varying content of BF reinforced PP composites; **(B)** SEM image of flexural fractured sample indicating crack propagation due to poor fiber matrix adhesion.

which undergoes further attrition during compounding and ECM. Yeole et al. (2021) observed ~97% reduction in fiber length of textile grade carbon fiber (TCF) while compounding with PP in twin screw extruder. Similarly, Alwekar et al. (2021) found 73–90% reduction in fiber length of glass fiber glass-PP long fiber thermoplastic composites manufacturing *via* ECM. Shear force due to screw rotation, fiber-fiber and fiber-matrix interaction are the major reasons for fiber attrition in the extrusion process (Yeole et al., 2020; Alwekar et al., 2021).

3.2.1.2 Flexural properties

Flexural properties of the natural fiber reinforced composites depend on the fiber content, fiber-matrix interfacial properties and processing condition(s) (Bajpai et al., 2012; Gholampour and Ozbakkaloglu, 2020). Flexural properties of PP with varying content of BF are presented in Figure 7A. Flexural properties of PP-BF composites exhibited similar trend as that of tensile properties. Figure 7A suggests that the 5 wt.% BF reinforced PP composites had maximum flexural strength (59.82 MPa), 64% increase compared to neat PP (36.40 MPa). On further increasing the BF content to 20wt%, the flexural strength decreased to 38.74 MPa however was still 6% higher than neat PP. The poor fiber matrix adhesion (as shown in Figures 6B1,B2) induces stress concentration in the composite and results in decreased flexural strength. Figure 7B illustrates the crack propagation due to fiber matrix debonding. Flexural modulus on the other hand increased till 15 wt.% addition of BF, and then decreased which can be attributed to porosity in the samples (Shibata et al., 2006) as observed in Figure 6B1.
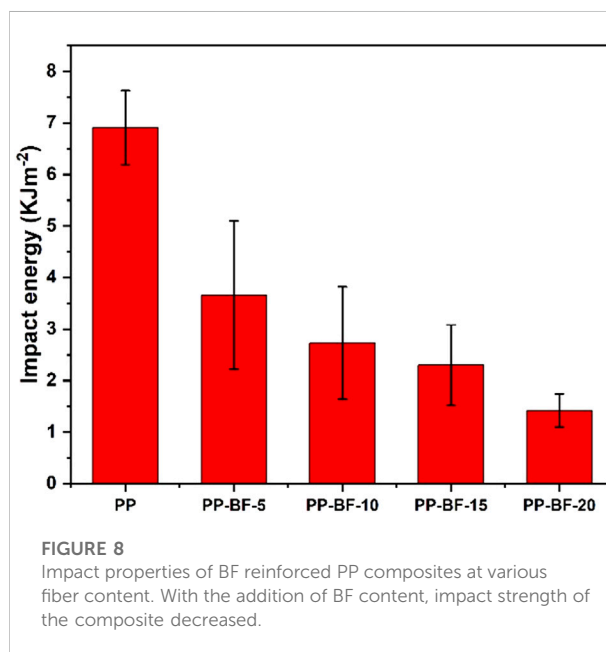

FIGURE 8
Impact properties of BF reinforced PP composites at various fiber content. With the addition of BF content, impact strength of the composite decreased.

3.2.1.3 Impact properties

The impact strength of fiber-reinforced polymer composites is influenced by the nature of the fiber, fiber length, fiber orientation, fiber content and fiber-matrix interface (Rahman et al., 2010; Kore et al., 2021). Figure 8 represents the trend of impact/break strength of PP-BF composites with varying content of BF. Neat PP exhibited the highest break strength of 6.91 kJ/m^2 due to the ductile nature of PP, which reduced by 79% to 1.42 kJ/m^2 for PP-BF-20. The low value of impact strength implies a lack of

resistance to sudden load. Fibers act as constraints resulting in a decrease in strain which reduces the resistance toward the sudden load. Bahari and Krause (2016) observed the decrease in impact strength with increase in BF content in bamboo-PVC composites. Mean charpy impact bending for neat PVC was 23 kJ/m^2 whereas that for BF-PVC with 25 and 50% loading was 3.8 kJ/m^2 and 0.7 kJ/m^2 respectively. However, Rahman et al. (2010) reported an increase in impact strength by 100 and 109% as compared to neat PP on adding both 30wt% treated and untreated saw dust content respectively in the PP matrix. Similarly, Mir et al. (2017) also observed increase in impact strength by ~15 and ~30% as compared in neat PP on adding 20wt% untreated and treated coir fibers respectively. A strong fiber-matrix interface was argued to provide effective resistance to crack propagation during sudden impact, and hence higher impact strength.

3.2.2 BS overmolded PP-BF composites

In a trailer, the decking is installed on a steel chassis frame. Therefore, the deck panels are subjected to three-point bend loading. Hence, flexure test is considered to be the most relevant/ significant test for this application. Cargo and dunnage are frequently fastened to the decking; hence nail pull-out is also a crucial test for truck decking.

3.2.2.1 Flexural properties

Average flexural strength and modulus of PP-BF-20 enhanced from 38.74 MPa and 1.27 GPa to 160.6 MPa and 28.4 GPa respectively on overmolding with BS. Huda et al. (2012) observed increase in flexural strength and modulus up to 50 and 60% on increasing BS concentration in PP matrix respectively, which decreased on further increasing the concentration of BS. The decline in strength and modulus on adding BS was due to the decrease in the adhesion between BS and PP resulting in failure due to BS-PP delamination (Huda et al., 2012). The flexural strength and modulus of PP-BF-BS panel was higher than that of commercially used Apitong for truck trailer applications. Apitong used for trailer decking application are reported to have 137.2 MPa and 14.3 GPa of flexural strength and modulus respectively (TrailerDecking, 2020–Wood Strength of Trailer Flooring).

3.2.2.2 Nail pull out test

The nail pull-out load of PP-BF-BS panel was 519 ± 163 N which was 10% lower than that of Apitong panel (579 ± 150 N). Figure 9A shows 3.785 mm diameter nail used for nail pull out test and Figures 9B,C Shows the hole left by nail pull out for Apitong and PP-BF-BS panel respectively. Apitong is a hardwood that contains natural oleoresin which helps to self-heal against the crack and damage (Our Apitong | terradeck. id). The dimension of the hole for Apitong was 3.785 mm (0.149 in), while for PP-BF-BS it was 3.556 mm

(0.140 in). A decrease in hole dimension for PP-BF-BS indicated self-healing behavior which is attributed to the ductile nature of PP (Slaven et al., 2022).

Three-point bend test results show that the PP-BF-BS have superior stiffness and strength compared to conventional Apitong decking. Apitong observed 10% higher nail pull out strength as compared to bamboo composite; however, self-healing property of PP-BF-BS showed promising results. Therefore, it was evident from the flexure and nail pull-out results that PP-BF-BS can be a replacement of Apitong.

4 Prototype PP-BF-BS deck

4.1 Prototype PP-BF-BS deck fabrication

Prototype PP-BF-BS decking was developed building upon the coupon level work presented earlier. A sandwich composite design approach (as explained earlier) was taken for the deck panel, where the core comprised continuous strips of bamboo over the entire length and the skins were produced by encapsulating ECM PP-BF. PP-BF pellets were compounded at Techmer PM, Clinton, Tennessee, USA as shown in Figure 10A. Figure 10B shows full-length bamboo strips that get placed as core in the deck panel mold. Having confirmed the wet-out and homogenous panel quality, the ECM process (as discussed in Section 2.2) was then used to produce ~200 PP-BF plates of 355 mm × 355 mm (14″x14″) with feedstock of compounded PP-BF pellets.

Welded steel elements were assembled to produce a two-cavity compression tool to fit a 75 metric ton compression Dake press (Dake Corporation, Grand Haven, Michigan, USA) equipped with 1.01 m × 1.01 m (40″x40″) platens. Cartridge heaters were added to the tool for heating. In addition, resistive heating via copper mesh placed between bamboo-skin and core layers was used for supplementary heating, to get heat to the core.

PP-BF skin (jacket) panels were butted against each other over the length of the tool, i.e., approximately 6-8 panels. Figure 11A depicts the BS and Figure 11B the skin panels respectively. The process conditions adopted were as follows. The top skin–core layup was heated for 1 h at 149°C, 30 min at 177°C, and 30 min at 191°C. The layup was pressed for 30 min and the heat was turned off and the part was allowed to cool to room temperature. The part was flipped and the lower skin-core was processed for 1 h at 149°C, 30 min at 177°C, and 30 min at 213°C. The part was pressed for 30 min, and the heat was turned off and cooled to room temperature under pressure. The total cycle time was ~4 h (not counting overnight cooling). The final PP-BF-BS plank geometry was ~63.5 mm (2.5″) thick, 1.21 m (4 ft) long. The PP-BF
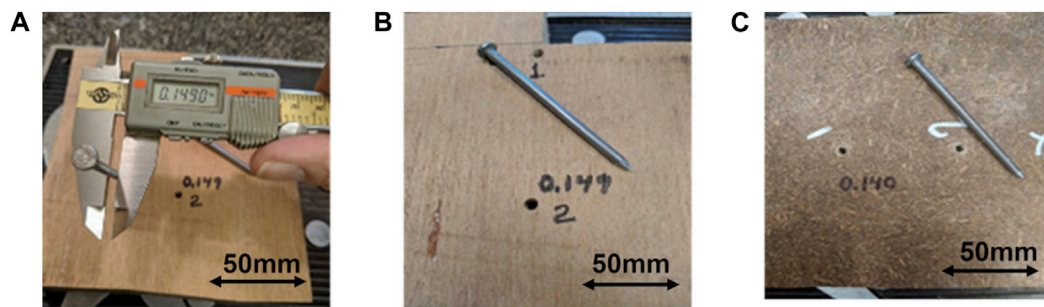
FIGURE 9
Dimensions of **(A)** nail used for nail pull out (nail diameter−3.785 mm) **(B)** hole made by nail after nail pull out test in Apitong (hole diameter−3.785 mm) **(C)** hole made by nail after nail pull out test in PP-BF-BS panel (hole diameter−3.556 mm).

FIGURE 10
Materials used in producing the sandwich PP-BF-BS; **(A)** Compounded 20% conditioned BF with PP; and **(B)** Solid strips approximately 3.2 m (10 ft) of bamboo core.

jacket (skin) was 12 mm (0.5″) (top and bottom) and 38.1 mm (1.5″) bamboo core. Despite these high temperatures, the planks exhibited some inconsistencies and small amount of degradation. This is attributed to the highly insulative nature of bamboo. With iterative process parameters, the panels were optimized to the extent possible within the constraints of the low-cost tool. The optimized final panels are illustrated in Figure 11C.

Molding Challenges: The mold design was not fully optimized for the proof-of-concept work. A gap between male and female allowed molten material to squeeze out. Several panels did not have optimal flow along the length and top. Some sectioned panels showed that PP did not fully flow into the bamboo core, which could need more detailed heating features in the tool which was not possible in the current proof-of-concept work. The copper mesh greatly improved heat flow into the part but had to be in direct contact with the tool surface to function effectively. The testing work progressed with realization that a production product would only provide much higher performance. Hence, the prototyping testing can be considered as highly conservative.

4.2 Prototype field testing and key observations

The deck beams shown in Figure 11C were field-tested by driving a Caterpillar CAT 349F (53.6 ton) cyclically (i.e., drive onto and off) a Magnitude 55-ton low boy. This test evaluates the planking toughness due to breakover impact and planking hardness due to grouser tractive forces. The planks were arranged on the frame according to the pattern shown in Figure 12. The PP-BF-BS decks are marked in the figure. Other deck elements comprised Apitong and other materials (not elaborated here).

Figure 13A provides visual indication of the treads (wear) after 60 cycles. Figure 13B illustrates the same after 80 cycles. It can be noted that the wear treads remain fairly similar despite increased number of cycles, indicating excellent material resistance to surface wear. The PP-BF-BS successfully withstood 400 load cycles (Slaven et al., 2022). The onset of failure was via microcracking and transverse cracking at the edges, where the plank was on supports to the frame as seen in Figure 13C. This represents a most aggressive form of loading. Notably the surface of the PP-BF-BS
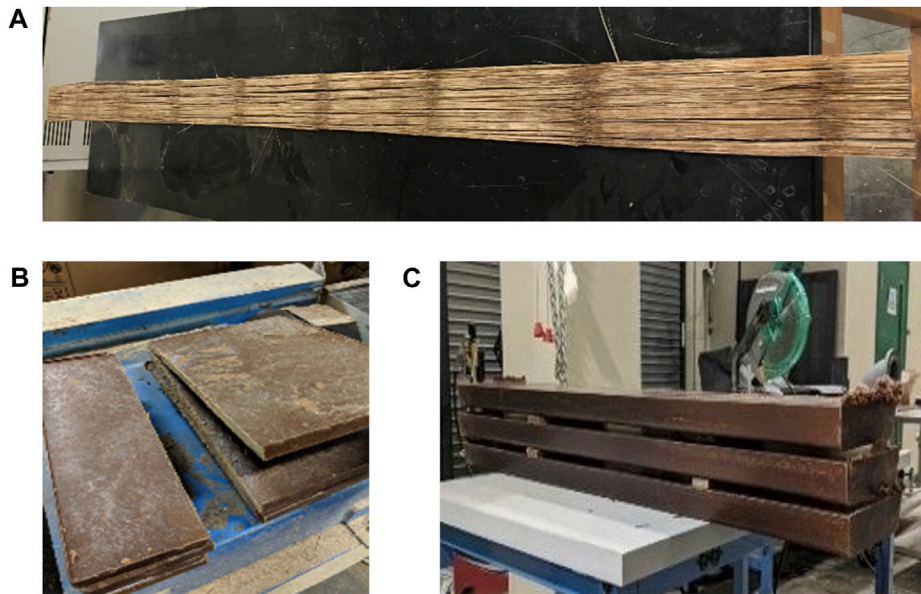
FIGURE 11
(A) BS used for core, **(B)** PP-BF skin; **(C)** optimized PP-BF-BS panel after processing. The dimension of the finished panels is 1.21 m × 0.355 m x 0.0635 m (48″x14″x2.5″).
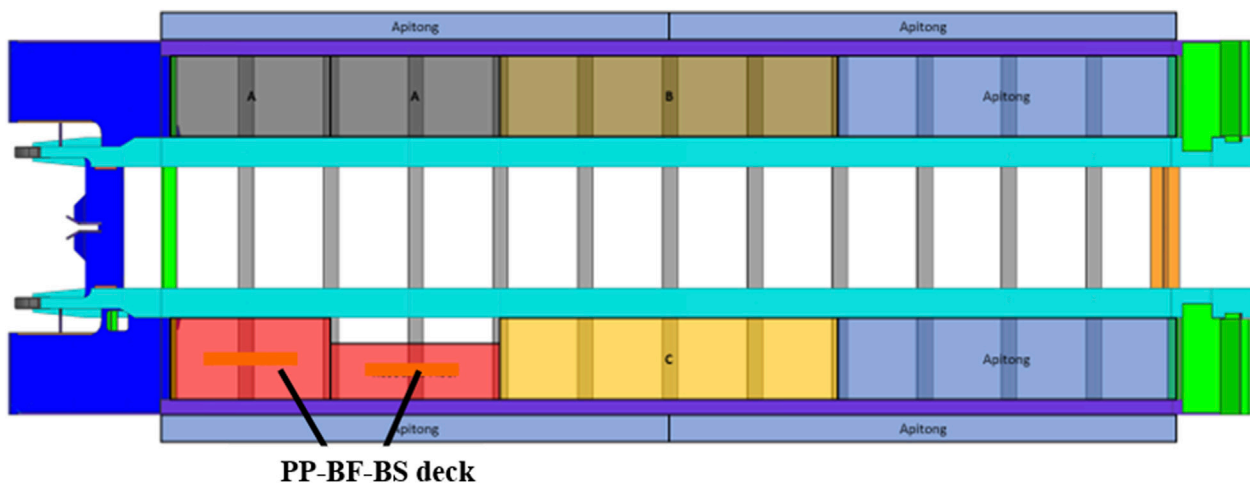

FIGURE 12
Arrangement of planks on the trailer frame. PP-BF-BS deck panels are marked in the figure. The other panels were made of other elements not discussed in this paper.

survived the track contacts as the vehicle moved in and out of the bed. Only pit marks were observed as seen in Figure 13B similar to that for Apitong and other materials (not elaborated here) that were included in the test.

Despite the process challenges such as heating through the thickness and less than optimal tool, the planks survived extreme loading conditions. With optimization of the BS core

to jacket interface and design of a production tool with optimal heating the plank quality would dramatically improve. This ought to limit the edge cracking. The surface texture and make-up of PP-BF ECM performed optimally, and no further optimization was deemed necessary. Table 2 presents the material ranking/scoring for PP-BF-BS compared to Apitong.
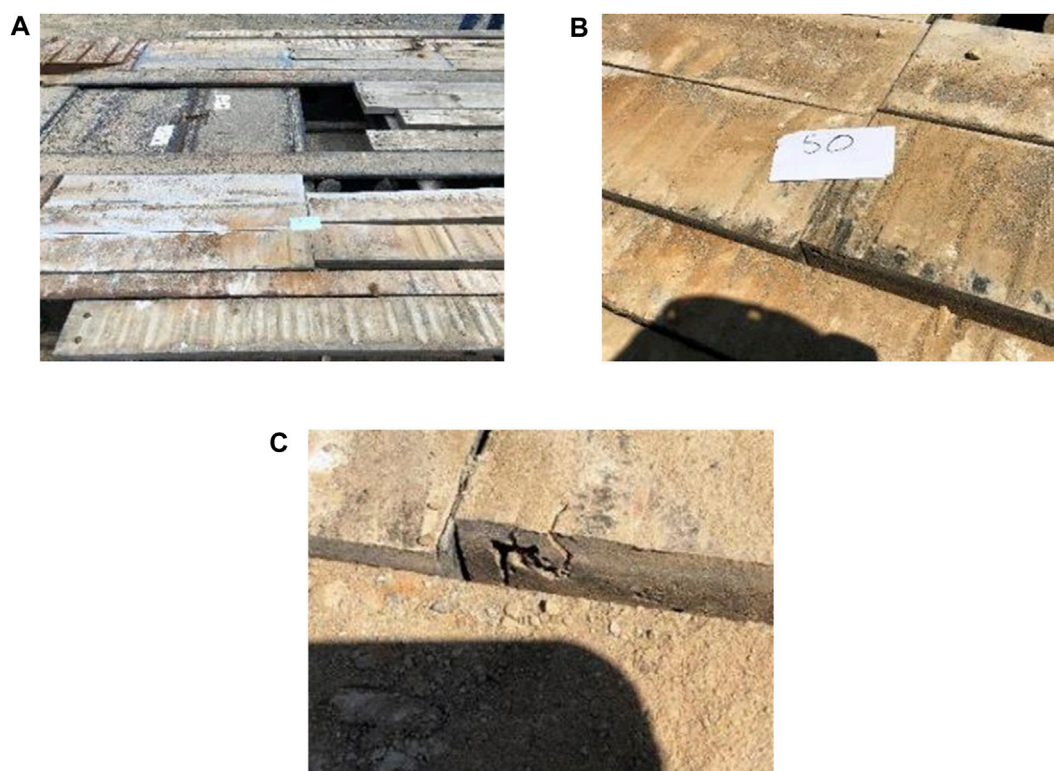
FIGURE 13
Tread wear; **(A)** Illustration of placement of the PP-BF-BS planks as explain before; **(B)** Tread marks due to several loading/unloading trials of driving the CAT over the planks back and forth; and **(C)** Localized cracking in the area of BS that had less binding to the jacket.

Discussion: The initial part of the work was primarily conducted to establish processing feasibility and mechanical properties of PP-BF composites. Through careful iterations the processing parameters such as temperature and pressure were established for the outer jacket (skin). The ECM approach was innovative and ideal to obtain uniform encapsulation of the strips. This is a scalable process for large panels in production. The core strips used in the prototype were in the as-received form (i.e., no attempt was made to further optimize them). Based on the field tests, the material withstood the extreme conditions effectively, and its performance can be further enhanced by designing the contact at the support points. This again is very scalable in production. Some studies have to be conducted for cost-effective surface treatment of the bamboo strips. Eventually the entire operation can be integrated in a 'pultrusion' type set up

where the jackets would be co-molded with the core (not part of the current scope).

5 Conclusion

5, 10, 15 and 20 wt.% BF were compounded with PP using twin-screw extruder and composites plaques were prepared via ECM technique. The addition of 20 wt.% BF showed 8% decrease in tensile strength; however, the modulus was increased by 85%. Poor fiber matrix interface was found in the SEM images. 20 wt.% BF reinforced PP was extrusion compression overmolded with BS to form trailer decks. BS overmolded PP-BF panel for trailer decking application had 15% higher flexural strength and 10% lower nail pull-out load as compared to apitong. PP-BF-BS panel also exhibited self-healing properties against the damage and cracks. Based on baseline work with PP-BF and PP-BF-BS composites, prototype of PP-BF-BS trailer decks of dimension 1.21 m × 0.355 m x 0.0635 m were fabricated, and field tested under aggressive loading conditions. PP-BF-BS decks survived 400 cycles of load with minimum damage. The primary damage mode was at the support locations to the frame which can be eliminated in a production design. The

TABLE 2 Material ranking/scoring for PP-BF-BS compared to Apitong Slaven et al., 2022.

Material	Apitong	PP-BF-BS
Surface	10	10
Bending	10	7[a]

[a]Process optimization can take this number to be comparable to Apitong.

PP-BF-BS as a material performed excellent in this application and is a viable alternative for Apitong.

Author's Note

Data availability statement

The partial datasets presented in this study can be found in IACMI technical report by Slaven et al. (2022) Website: http://www.osti.gov/scitech/.

Author contributions

SW—Bamboo-PP ECM trials and writing sections of the manuscript; SK–Testing, nail pull out and writing sections of the manuscript; PY—ECM process, data curation, editing; HT–Panel production support; SO–Editing and supervision; UV—Writing sections of field testing, supervision, funding, editing.

Funding

Acknowledgments

Conflict of interest

The authors declare that the research was conducted in the absence of any commercial or financial relationships that could be construed as a potential conflict of interest.

Publisher's note

All claims expressed in this article are solely those of the authors and do not necessarily represent those of their affiliated organizations, or those of the publisher, the editors and the reviewers. Any product that may be evaluated in this article, or claim that may be made by its manufacturer, is not guaranteed or endorsed by the publisher.

References

Abdul Khalil, H. P. S., Bhat, I. U. H., Jawaid, M., Zaidon, A., Hermawan, D., and Hadi, Y. S. (2012). Bamboo fibre reinforced biocomposites: A review. *Mat. Des.* 42, 353–368. doi:10.1016/j.matdes.2012.06.015

Ali, H. T., Akrami, R., Fotouhi, S., Bodaghi, M., Saeedifar, M., Yusuf, M., et al. (2021). Fiber reinforced polymer composites in bridge industry. *Structures* 30, 774–785. doi:10.1016/j.istruc.2020.12.092

Aliyeva, N., Sas, H. S., and Saner Okan, B. (2021). Recent developments on the overmolding process for the fabrication of thermoset and thermoplastic composites by the integration of nano/micron-scale reinforcements. *Compos. Part A Appl. Sci. Manuf.* 149, 106525. doi:10.1016/j.compositesa.2021.106525

Alwekar, S., Yeole, P., Kumar, V., Hassen, A. A., Kunc, V., and Vaidya, U. K. (2021). Melt extruded versus extrusion compression molded glass-polypropylene long fiber thermoplastic composites. *Compos. Part A Appl. Sci. Manuf.* 144, 106349. doi:10.1016/j.compositesa.2021.106349

Bahari, S. A., and Krause, A. (2016). Utilizing Malaysian bamboo for use in thermoplastic composites. *J. Clean. Prod.* 110, 16–24. doi:10.1016/j.jclepro.2015.03.052

Bajpai, P. K., Singh, I., and Madaan, J. (2012). Comparative studies of mechanical and morphological properties of polylactic acid and polypropylene based natural fiber composites. *J. Reinf. Plast. Compos.* 31, 1712–1724. doi:10.1177/0731684412447992

Chee, S. S., Jawaid, M., Sultan, M. T. H., Alothman, O. Y., and Abdullah, L. C. (2019). Thermomechanical and dynamic mechanical properties of bamboo/woven kenaf mat reinforced epoxy hybrid composites. *Compos. Part B Eng.* 163, 165–174. doi:10.1016/j.compositesb.2018.11.039

Chin, S. C., Tee, K. F., Tong, F. S., Ong, H. R., and Gimbun, J. (2020). Thermal and mechanical properties of bamboo fiber reinforced composites. *Mat. Today Commun.* 23, 100876. doi:10.1016/j.mtcomm.2019.100876

Das, M., and Chakraborty, D. (2008). Evaluation of improvement of physical and mechanical properties of bamboo fibers due to alkali treatment. *J. Appl. Polym. Sci.* 107, 522–527. doi:10.1002/app.26155

Deshpande, A. P., Bhaskar Rao, M., and Lakshmana Rao, C. (2000). Extraction of bamboo fibers and their use as reinforcement in polymeric composites. *J. Appl. Polym. Sci.* 76, 83–92. doi:10.1002/(sici)1097-4628(20000404)76:1<83::aid-app11>3.0.co;2-l

Duflou, J. R., Deng, Y., Van Acker, K., and Dewulf, W. (2012). Do fiber-reinforced polymer composites provide environmentally benign alternatives? A life-cycle-assessment-based study. *MRS Bull.* 37, 374–382. doi:10.1557/mrs.2012.33

Fang, H., Sun, H., Liu, W., Wang, L., Bai, Y., and Hui, D. (2015). Mechanical performance of innovative GFRP-bamboo-wood sandwich beams: Experimental and modelling investigation. *Compos. Part B Eng.* 79, 182–196. doi:10.1016/j.compositesb.2015.04.035

Gholampour, A., and Ozbakkaloglu, T. (2020). *A review of natural fiber composites: Properties, modification and processing techniques, characterization, applications.* US: Springer. doi:10.1007/s10853-019-03990-y

Global Truck (2022). *Trailer market to 2026 - by application type, truck tonnage capacity, trailer type, vehicle type and region.* Available at: https://www.prnewswire.com/news-releases/global-truck-trailer-market-to-2026—by-application-type-truck-tonnage-capacity-trailer-type-vehicle-type-and-region-301484696.html (Accessed June 8, 2022).

Guo, J., Cao, M., Ren, W., Wang, H., and Yu, Y. (2021). Mechanical, dynamic mechanical and thermal properties of TiO2 nanoparticles treatment bamboo fiber-reinforced polypropylene composites. *J. Mat. Sci.* 56, 12643–12659. doi:10.1007/s10853-021-06100-z

Hexcel.com (2022). Honeycomb sandwich design Technology - hexcel.com. Available at: https://www.yumpu.com/en/document/read/22265594/honeycomb-sandwich-design-technology-hexcelcom (Accessed June 12, 2022).

Hidalgo-Salazar, M. A., and Correa, J. P. (2018). Mechanical and thermal properties of biocomposites from nonwoven industrial fique fiber mats with epoxy resin and linear low density polyethylene. *Results Phys.* 8, 461–467. doi:10.1016/j.rinp.2017.12.025

Huda, S., Reddy, N., and Yang, Y. (2012). Ultra-light-weight composites from bamboo strips and polypropylene web with exceptional flexural properties. *Compos. Part B Eng.* 43, 1658–1664. doi:10.1016/j.compositesb.2012.01.017

Ibrahim, I. D., Jamiru, T., Sadiku, R. E., Kupolati, W. K., Agwuncha, S. C., and Ekundayo, G. (2015). The use of polypropylene in bamboo fibre composites and their mechanical properties - a review. *J. Reinf. Plast. Compos.* 34, 1347–1356. doi:10.1177/0731684415591302

Khademibami, L., Sherrington, A., Shmulsky, R., and Quin, F. (2021). Determination of flexural strength of structural red and white Oak and hardwood composite lumber. *For. Prod. J.* 71, 401–406. doi:10.13073/fpj-d-21-00051

Slaven, L., Knight, D., Vaidya, U., Drzal, L. T., Unser, J., Ozcan, S., et al. (2022). Bamboo bio-composite truck / trailer decking. Available at: http://www.osti.gov/scitech/.

Kore, S., Spencer, R., Ghossein, H., Slaven, L., Knight, D., Unser, J., et al. (2021). Performance of hybridized bamboo-carbon fiber reinforced polypropylene composites processed using wet laid technique. *Compos. Part C. Open Access* 6. doi:10.1016/j.jcomc.2021.100185100185)

Lee, S.-Y., Kang, I.-A., Park, B.-S., Doh, G.-H., and Park, B.-D. (2009). Effects of filler and coupling agent on the properties of bamboo fiber-reinforced polypropylene composites. *J. Reinf. Plast. Compos.* 28, 2589–2604. doi:10.1177/0731684408094070

Lotfi, A., Li, H., Dao, D. V., and Prusty, G. (2021). Natural fiber–reinforced composites: A review on material, manufacturing, and machinability. *J. Thermoplast. Compos. Mater.* 34, 238–284. doi:10.1177/0892705719844546

Mir, S. S., Hasan, M., Hasan, S. M. N., Hossain, M. J., and Nafsin, N. (2017). Effect of chemical treatment on the properties of coir fiber reinforced polypropylene and polyethylene composites. *Polym. Compos.* 38, 1259–1265. doi:10.1002/pc.23690

Mohanty, A. K., Vivekanandhan, S., Pin, J. M., and Misra, M. (2018). Composites from renewable and sustainable resources: Challenges and innovations. *Science* 362, 536–542. doi:10.1126/science.aat9072

Mousavi, S. R., Zamani, M. H., Estaji, S., Tayouri, M. I., Arjmand, M., Jafari, S. H., et al. (2022). Mechanical properties of bamboo fiber-reinforced polymer composites: A review of recent case studies. *J. Mat. Sci.* 57, 3143–3167. doi:10.1007/s10853-021-06854-6

Ning, H., Lu, N., Hassen, A. A., Chawla, K., Selim, M., and Pillay, S. (2020). A review of Long fibre thermoplast (LFT) composites. *Int. Mat. Rev.* 65, 164–188. doi:10.1080/09506608.2019.1585004

Osei-Antwi, M., De Castro, J., Vassilopoulos, A. P., and Keller, T. (2014). Structural limits of FRP-balsa sandwich decks in bridge construction. *Compos. Part B Eng.* 63, 77–84. doi:10.1016/j.compositesb.2014.03.027

Rahman, M. R., Islam, M. N., and Huque, M. M. (2010). Influence of fiber treatment on the mechanical and morphological properties of sawdust reinforced polypropylene composites. *J. Polym. Environ.* 18, 443–450. doi:10.1007/s10924-010-0230-z

Rajendran Royan, N. R., Leong, J. S., Chan, W. N., Tan, J. R., and Shamsuddin, Z. S. B. (2021). *Current state and challenges of natural fibre-reinforced polymer composites as feeder in fdm-based 3d printing*, 13. doi:10.3390/polym13142289Polym. (Basel)

Rassiah, K., Ahmad, M. M. H. M., and Ali, A. (2014). Mechanical properties of laminated bamboo strips from Gigantochloa Scortechinii/polyester composites. *Mat. Des.* 57, 551–559. doi:10.1016/j.matdes.2013.12.070

Ratna Prasad, A. V., and Mohana Rao, K. (2011). Mechanical properties of natural fibre reinforced polyester composites: Jowar, sisal and bamboo. *Mat. Des.* 32, 4658–4663. doi:10.1016/j.matdes.2011.03.015

Shibata, S., Cao, Y., and Fukumoto, I. (2006). Lightweight laminate composites made from kenaf and polypropylene fibres. *Polym. Test.* 25, 142–148. doi:10.1016/j.polymertesting.2005.11.007

Terradeck (2022). Our Apitong | terradeck.id. Available at: https://terradeck.id/ourapitong (Accessed May 10, 2022).

Thwe, M. M., and Liao, K. (2003). Durability of bamboo-glass fiber reinforced polymer matrix hybrid composites. *Compos. Sci. Technol.* 63, 375–387. doi:10.1016/s0266-3538(02)00225-7

TrailerDecking (2022). TrailerDecking.com - wood strength of trailer flooring. Available at: https://www.trailerdecking.com/wood-charts.aspx (Accessed May 10, 2022).

Wang, Q., Jones, J., Lu, N., Johnson, R., Ning, H., and Pillay, S. (2018). Development and characterization of high-performance kenaf fiber–HDPE composites. *J. Reinf. Plast. Compos.* 37, 191–200. doi:10.1177/0731684417739127

Wei, Y., Chen, S., Jiang, J., Zhou, M., and Zhao, K. (2022). Experimental investigation of bamboo-concrete composite beams with threaded reinforcement connections. *Jnl. Sandw. Struct. Mater.* 24, 601–626. doi:10.1177/10996362211023529

Yeole, P., Alwekar, S., Veluswamy, N. K. P., Kore, S., Hiremath, N., Vaidya, U., et al. (2021). Characterization of textile-grade carbon fiber polypropylene composites. *Polym. Polym. Compos.* 29, 652–659. doi:10.1177/0967391120930109

Yeole, P., Hassen, A. A., Kim, S., Lindahl, J., Kunc, V., Franc, A., et al. (2020). Mechanical characterization of high-temperature carbon fiber-polyphenylene sulfide composites for large area extrusion deposition additive manufacturing. *Addit. Manuf.* 34. doi:10.1016/j.addma.2020.101255101255)

Yeole, P., Ning, H., Hassen, A. A., and Vaidya, U. K. (2018). The effect of flocculent, dispersants, and binder on wet–laid process for recycled glass fiber/PA6 composite. *Polym. Polym. Compos.* 26, 259–269. doi:10.1177/096739111802600306

Yusoff, M. S. R., Bahari, S. A., Haliffuddin, R. M. A. A., Zakaria, M. N., Jamaluddin, M. A., and Rashid, N. H. M. N. (2021). Chemical contents and thermal stability of Madu bamboo (Gigantochloa albociliata) for natural-bonded fiber composites. *IOP Conf. Ser. Earth Environ. Sci.* 644, 012009. doi:10.1088/1755-1315/644/1/012009

Zhang, K., Wang, F., Liang, W., Wang, Z., Duan, Z., and Yang, B. (2018). Thermal and mechanical properties of bamboo fiber reinforced epoxy composites. *Polym. (Basel)* 10, 608. doi:10.3390/polym10060608